Grant Agreement No.: 226479

SafeLand

Living with landslide risk in Europe: Assessment,
effects of global change, and risk management strategies

7th Framework Programme
Cooperation Theme 6 Environment (including climate change)
Sub-Activity 6.1.3 Natural Hazards

Deliverable 3.7

Expected changes in climate-driven landslide activity (magnitude, frequency) in Europe in the
next 100 years

Work Package 3.3 - Landslide risk evolution in selected "hotspots" areas

Deliverable/Work Package Leader: ICG   Revision: Final

July, 2011

Rev.	Deliverable Responsible	Controlled by	Date
0	ICG	JRC	12.08.2011
1			
2			

SUMMARY

Earlier studies within the Safeland project (D2.10) have shown that landslides currently threaten approximately 3.5 to 7 million people in Europe. A significant amount of infrastructure is also exposed.

Landslide hazard level is expected to change in a changing climate. Landslide vulnerability will also change with societal and demographic development. This study explores the possible evolution in both landslide hazard and risk within the next 80 years. Predicted precipitation pattern, and expected changes in land cover and population are used as input to access the landslide hazard and risk in the years 2030, 2050, 2070 and 2090. The results are compared to the present state in 2010.

The study shows that only minor variations are expected in landslide hazard level. The total amount of land area exposed to landslides will increase by 1.5%. The increase in risk is lower and amounts to 0.7% of the total European population. Some countries might experience a reduction in the total exposed population, while others can expect an increase of 2 to 10% (e.g. Italy -0.9%, Switzerland +2.9, Macedonia +11.0%).

Note about contributors

The following organizations contributed to the work described in this deliverable:

Lead partner responsible for the deliverable:
Christian Jaedicke, ICG
Kjetil Sverdrup-Thygeson, ICG
Egil Syre, ICG
Farrokh Nadim, ICG
Bjørn Kalsnes, ICG
Bjørn Vidar Vangelsten, ICG

Partner responsible for quality control:
Javier Hervás, JRC
Miet Van Den Eeckhaut, JRC

Other contributors:
Christine Radermacher, MPG
Guenther Fischer, IIASA

CONTENTS

1   INTRODUCTION

Earlier in the SafeLand project hotspots of landslide hazard and risk have been identified (Work Package 2.4, D2.10, Jaedicke et al., 2011). For this purpose three independent models, all based on the same input data, were developed. The analysis covered all of Europe, such that differences between regions and countries in Europe could be identified. This homogenous analysis allowed comparing and ranking European countries in absolute or relative numbers for exposed land area, population and infrastructure. All risk models ranked Italy as the country with the highest total exposure. In terms of relative exposure compared to their total land area and population, the small alpine countries ranked highest. Detailed results are presented in SafeLand deliverable D2.10.

In the expectation of a global climate change, the question arises how the current level of landslide hazard and risk in Europe will evolve in the next 90 years (until 2100). Here several aspects play a role. Not only the climate, but also the demography and land cover in Europe will change. Prognosis needs to take into account a possible reduction in the total population and expected urbanisation in most parts of Europe. This again leads to a change in land cover where for example the amount of forested areas and urban areas may change dramatically.

The effect of climate change on landslide hazard varies depending on the type of landslide. In this study the focus is on precipitation-induced landslides. They are a direct consequence of extreme precipitation events and therefore closely coupled to a change in the number of such extreme events. Other landslides caused by drought or melt-freeze cycles (e.g. rock falls) often follow a complex sequence of weather events that are difficult, if not impossible to forecast, and are therefore not considered in this study.

The availability of homogenous European hazard and vulnerability related datasets is essential. For the future scenarios the same dataset needs to be available for selected points in time. The study uses the model developed by ICG in SafeLand deliverable D2.10 to model the reference state of landslide hazard and risk at present (2010). The model is then applied for the years 2030, 2050, 2070 and 2090.

The objectives of this study are to quantify landslide hazard and risk in Europe now and in the future and see if there will be significant changes. The study documents where the changes are expected to be most prominent and if there is a decrease or increase in risk when the changing demography is taken into account. Finally, the results of the study are compared and discussed in comparison to findings in SafeLand deliverable D2.10.

2   MATERIALS AND METHODS

2.1   INPUT DATA

The input data for the applied model are described in detail in SafeLand deliverable D2.10. In this analysis the following datasets from the overview in D2.10 are used: topography and geology. These environmental characteristics are assumed to remain constant in a changing climate.

Three additional datasets, different than those used in D2.10 are introduced in this study: Precipitation, population and land cover.

2.1.1   Precipitation

In the landslide hazard model produced for 2010 in D2.10, a monthly global dataset for the precipitation was used to estimate the expected extreme monthly precipitation (Global Precipitation Climatology Centre, Deutscher Wetterdienst, Offenbach, Germany). This dataset is now replaced with model results of the REMO model operated by the Max Planck Institute in Hamburg (Jacob 2001, Jacob et al. 2001). The model was first used in a control run to recalculate the current climate in the period 1981 to 2000. The same model was then applied to estimate the climate evolution in Europe until 2100. The model uses the A1B scenario defined by the IPCC (IPCC, 2007) and the boundary conditions for the regional model are defined by the global ECHAM5 model. Spatial resolution of the model is 25×25km. The model is described in detail in D3.1.

The IPCC A1 scenarios are based on the assumptions of continuing and rapid economic growth, a global population that peaks in mid-century and rapid introduction of new and more efficient technologies. A1 is divided into three groups that describe alternative directions of technological change where (A1B) presents a balance between fossil intensive and non-fossil energy resources.

To get an estimate of the extreme precipitation events, the 99.9% percentile of daily precipitation was calculated for 20 year periods from 1981-2100. This value represents the amount of daily precipitation that is exceeded every 50 years in the grid cell, and ranges from 26 mm to 1557 mm.

The data are reclassified to be used in the landslide hazard model (Table 2-1) using a logarithmic classification scale. Figure 2-1 shows the development of the 99.9% percentile of precipitation in Europe for 20-year intervals from 2000 to 2100. 0.1% of all precipitation events in a 20-year period are higher than the pixel values in the maps.

Table 2-1: Reclassification for 99.9% percentile of precipitation extremes in Europe

Daily (24h) precipitation in millimeters	Susceptibility	Tp_1
0 – 60	Low	1
61 – 75	Moderate	2
76 – 95	Medium	3
96 – 120	High	4
> 120	Very high	5
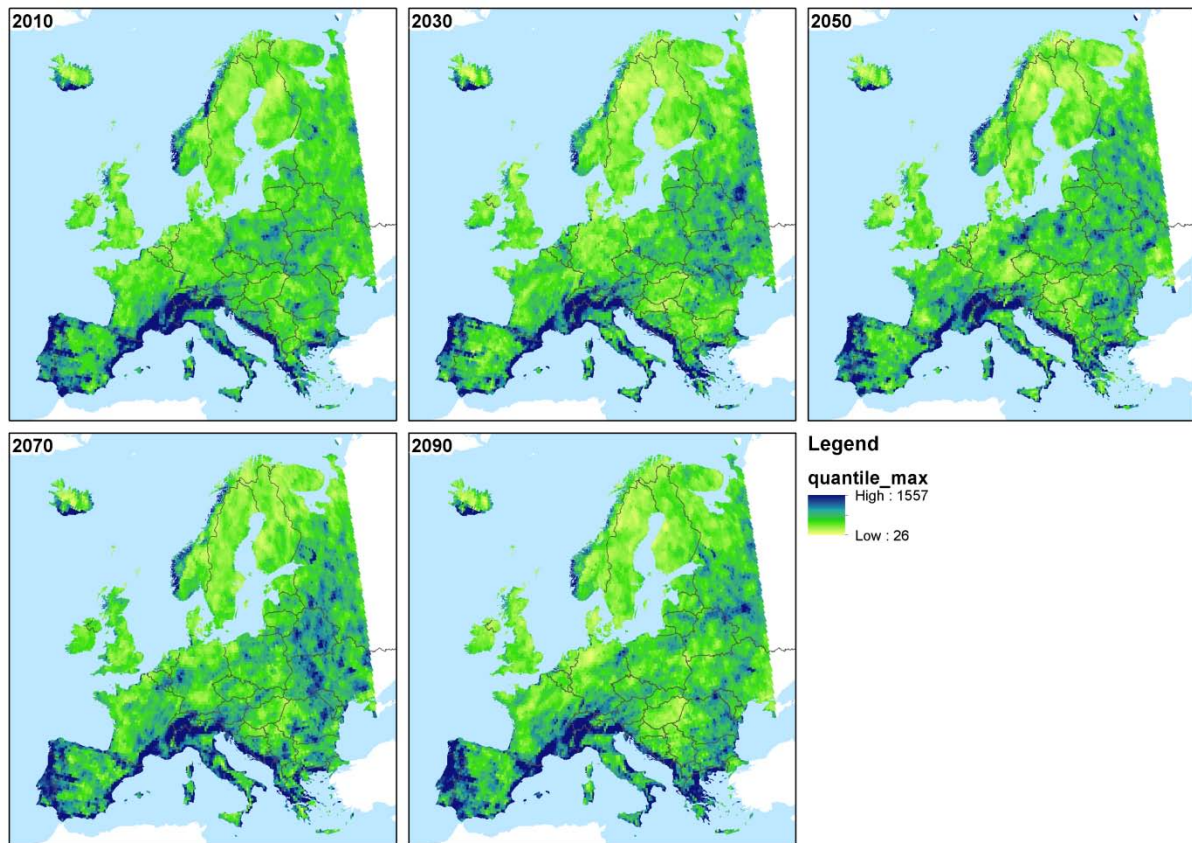
Figure 2-1: Absolute value of the 99.9% percentile of precipitation in Europe. 0.1% of all precipitation events in a 20 year period are higher than the pixel values in the maps. Each map represents a 20 year period (e.g. 2000-2020 is represented by 2010). Highest precipitation extremes are found in the Mediterranean, Iceland and Norway. The trend in the future is towards more extreme events in the south, while they decrease slightly in the North

2.1.2 Land cover

Land cover will change with changing climate and demography. This is mainly of importance for growing urban areas and the development of forested area in Europe. The applied land cover data were produced by The International Institute for Applied Systems Analysis (IIASA) based on the A2 scenario of the IPCC assessment report. The A2 describes a very heterogeneous world with high population growth, slow economic development and slow technological change. This scenario gives similar climate signals as the A1B used in the precipitation data until ca. 2060.

Tubiello and Fischer (2007) described the dataset as follows: *"The simulation tool IISASA-FAO AWZ model uses detailed agronomic based knowledge to simulate availability and use of land resources, farm-level management options, and crop production potentials as a function of climate. At the same time, it employs detailed spatial biophysical and socio-economic data sets to distribute its computations at fine gridded intervals over the entire globe (Fischer et al, 2002).*

Specifically, AEZ employs the FAO-UNESCO Digital Soil Map of the World (DSMW) as the underlying reference for its own land-surface database, which consists of more than 2.2 million grid cells at 5' latitude x 5' longitude (i.e., with a size of about 10 x 10 km at the equator). In

addition, a global digital elevation map (DEM) and derived slope distribution database are linked to DSMW. AEZ's current climate database is based on datasets developed by the Climate Research Unit (CRU, University of East Anglia). These comprise historical monthly mean data for the period 1901-1996 and include a monthly mean climatology (e.g., that describes mean monthly minimum temperature, mean monthly maximum temperature, precipitation, wet-day frequency, cloudiness, vapor pressure deficit) based on the decades 1961-1990 (New et al, 1998). In AEZ, the CRU data are transformed into daily data and analyzed vis-a-vis crop requirements (Fischer et al, 2002).

Finally, AEZ employs a land cover/land use layer that specifies distributions of aggregate land-cover classes, as derived from global-km land-cover datasets from, respectively, National Oceanic and Atmospheric Administration Advanced Very High Resolution Radiometer (NOAA AVHRR; see http://edcsnsI7.cr.usgs.gov/glcc/globdoc2_0.htmlfor details) and Global Landcover Classification (GLC2000; see http ://www-gvm.jrc.itlglc2000/ for details). Based on these spatial land-cover data sets and consistent with land statistics from the FAO statistics database (FAOSTAT), the AEZ global land-resources database incorporates spatial delineation and accounting of forest and protected areas. In terms of key socio-economic datasets, AEZ employs a global population data set calibrated for the year 2000, including estimates of spatially explicit population distributions and densities for each country at 5' latitude $\times$ 5' longitude" (grid size of ca 10 km at the equator)

The IIASA data give a percentage of land cover for 6 classes, e.g. 6 different maps. To achieve one grid for land cover in Europe, the class with the highest percentage in each grid cell was selected to represent the grid cell in the calculations. For example if the grid cell would show (10% cropland, 10% forest, 30% grassland, 0% urban, 10% other, 40% water), the grid cell would be represented as water in the further analysis.

The data is then reclassified according to the susceptibility of the different land cover classes to landsliding (Table 2-2). Figure 2-2 shows the expected development of land cover in Europe during the coming 100 years.

Close to the coast, highly populated and other areas were often classified as not susceptible since most of a typical grid cell would consist of water. To avoid this error, water was completely removed from the land cover analysis. In this way, the next highest percentage would be chosen for such a grid cell (grassland in the example). Water bodies are later assigned zero susceptibility due to zero terrain steepness. Since the terrain model features a much higher resolution, the accuracy in coastal areas is increased by this method.

Table 2-2: Reclassification for land cover. The applied vegetation cover factors S_v increase the susceptibility for surfaces that are easily eroded and reduce it in forested and urban areas. For urban areas, the positive effects of soil stabilization by constructions and water management are assumed to be dominant over the effects of negative of human activities.

Land cover class	Susceptibility	S_v
Water	Ignored	
Urban	Moderate	0.5
Forest	Medium	0.9
Cropland	High	1.1
Grassland	Very high	1.2
Other (mainly barren and water)	Very high	1.2
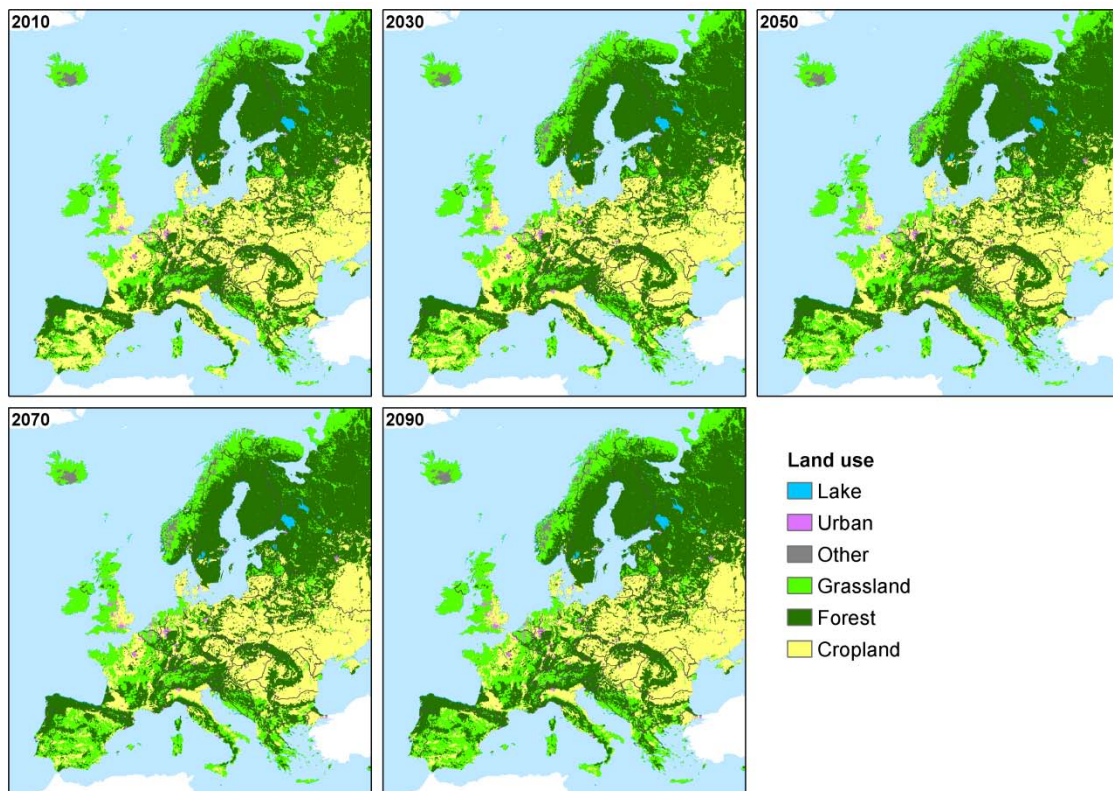
Figure 2-2: Development of land cover in Europe. The data is based on (IIASA, 2010). Predicted changes in land cover are small, but some changes from cropland to grassland in Spain and Italy can be observed.

2.1.3   Population

The population distribution will change significantly in Europe in the next 100 years. Also this dataset was developed by The International Institute for Applied Systems Analysis (IIASA) based on the A2 scenario of the IPCC assessment report.

The same model as described in Section 2.1.2, the IISASA-FAO AWZ model is used to estimate the development of the global population (Tubiello and Fischer, 2007). The basis is the global population for the year 2000 which is then adjusted with climate and socio-economic forcing of the AWZ model.

Figure 2-3 show the population density in year 2010 and the change in relation to 2010 for the years 2030, 2050, 2070 and 2090.
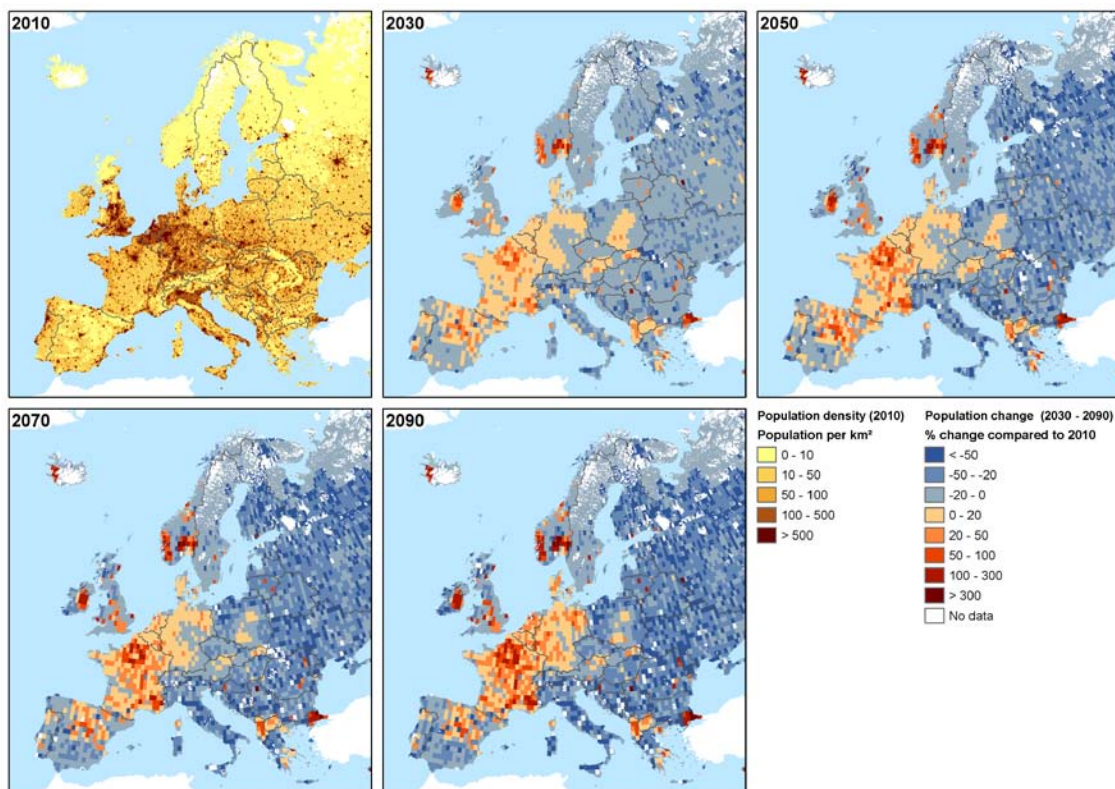
Figure 2-3: Population density in 2010 and its relative changes in percent compared to 2010. Generally, one can observe that large cities grow and the population in eastern Europe decreases, while it increases in western Europe.

2.2   THE LANDSLIDE HAZARD MODEL

In the hotspot study for SafeLand deliverable D2.10, three landslide hazard models were tested and compared. Models were developed by the Joint Research Centre (JRC), University of Lausanne (UNIL) and the International Centre for Geohazards (ICG). The ICG and JRC models compared well and reproduced the same pattern of landslide hazard and risk in Europe. The UNIL model considered only rockfalls, and was not compared to the other models. This is the reason why only one model (ICG, Figure 2-4) was chosen for the future climate change analysis. The topography and geology input data sets are assumed to be climate independent and are kept static. Precipitation, land cover and population are changed according to climate change scenarios A1B or A2.

Each input dataset is reclassified with respect to its effect on landslide hazard according to expert experience.

For the estimation of landslide risk, the resulting hazard maps are coupled with the population map of the same time period. The amount of people in each hazard class are counted and listed for each country. To calculate the "exposed" population the four hazard classes were weighted according to:

$$\text{exposed} = 1.0 \times \text{high} + 0.3\ \text{medium} + 0.1\ \text{low} + 0.0\ \text{negligible}$$

Details about the model can be found in SafeLand deliverable D2.10 and in the annex of this deliverable. A general discussion of the model approach is available in Nadim et al. (2006).
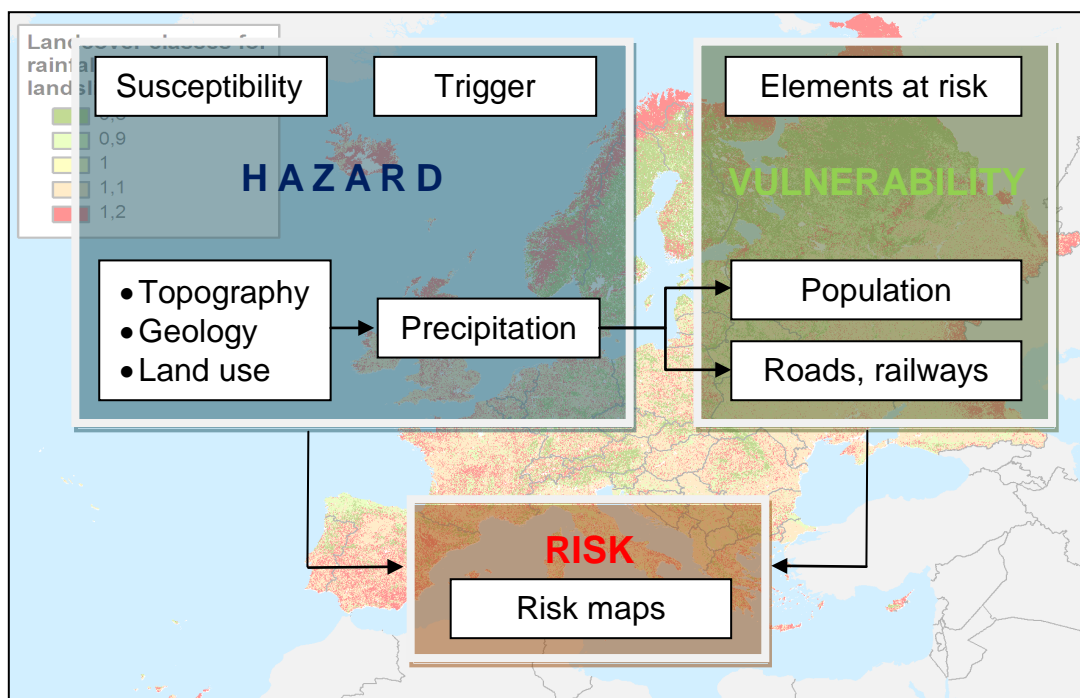
Figure 2-4: Schematic approach for landslide hazard and risk evaluation. In the present study only the precipitation trigger is used.

3   RESULTS

3.1   LAND COVER

Land cover is one of the factors that contributes to landslide susceptibility together with topography and geology. While topography and geology are assumed to remain constant during the next 100 years, land cover will most likely be altered by a changing climate and demography.

Changes in land cover are mainly caused by two processes, urbanization and a change in agricultural practices in different parts of Europe. It can be easily seen from the map in Figure 3-1 that some major cities such as London or Malmö in Sweden are growing. The biggest changes are visible in Spain, France and Germany where much of the current farmland is turned into grassland (destabilization) or forested areas (stabilization) in the future scenarios.

Land cover has a limited effect on the overall landslide hazard, but forested areas are less susceptible for landslides than croplands or pasture. Therefore a conversion to forest will lead to a stabilization of presently unstable slopes.
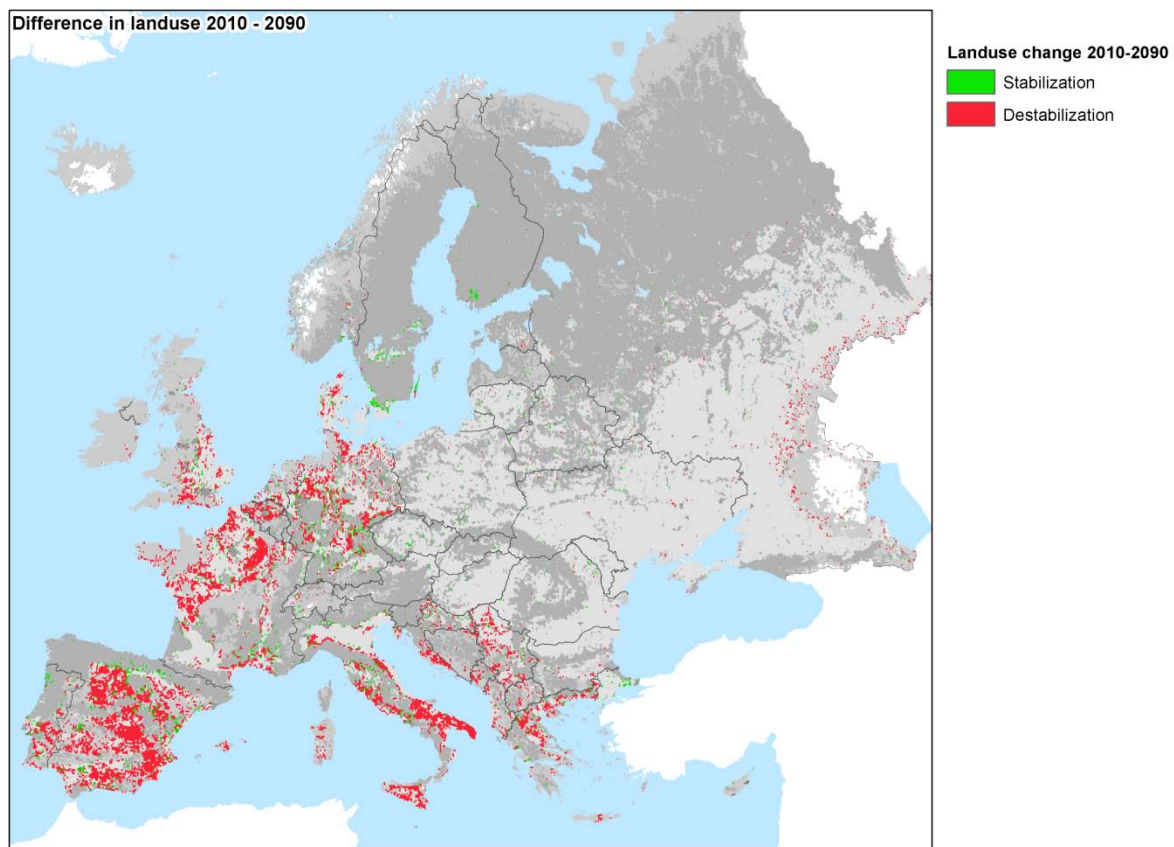
Figure 3-1: Change of land cover from 2010 to 2090. Red pixels show areas where the land cover is changing in a future climate scenario.

3.2   PRECIPITATION

To calculate hazard from susceptibility a trigger process is needed. In this study only precipitation as a trigger is considered. Both the normal mean and extreme precipitation events influence the triggering of landslides.

Figure 3-2 shows the evolution of the 99.9% percentile of daily precipitation relative to the 2010 situation. There is a clear positive trend in the daily precipitation extremes on Iberia, central Europe and Greece. Here, precipitation of short duration and high intensity will increase, while the changes further north are much less obvious. Decreasing annual precipitation seems to lead to more extreme events. This can also be seen in the more continental areas of Ukraine, Belarus and Russia. The model predicts very little change in other countries, for example Hungary.

Also the total amount of rainfall (Figure 3-3) shows a similar trend. More rain in the north and less in the southern parts of Europe is expected from climate model results. It should be noted that this analysis is based on daily precipitation values that do not always represent intensive convective showers with only short duration such as thunder storms.
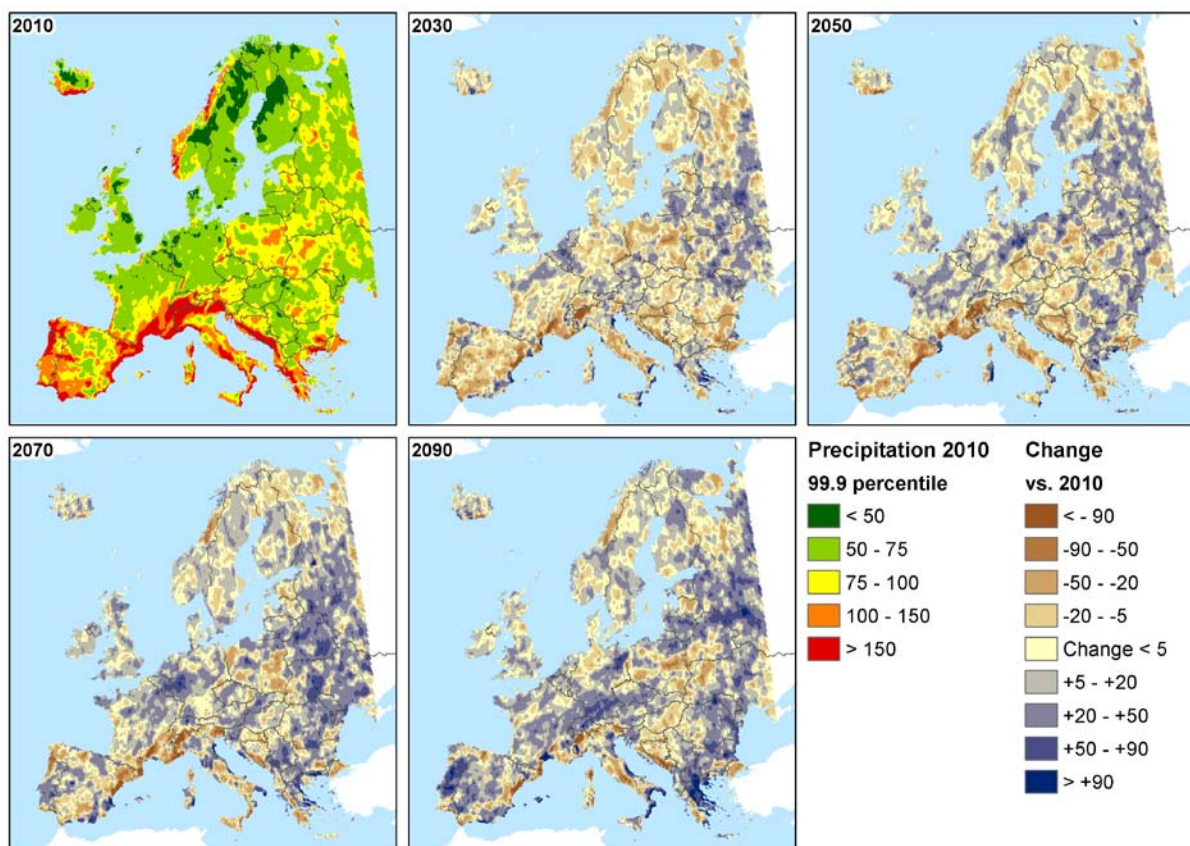
Figure 3-2: Changes in the 99.9% percentile 2010 – 2090 relative to the 2010 situation. More extreme events can be expected mostly on Iberia, central Europe and Greece.
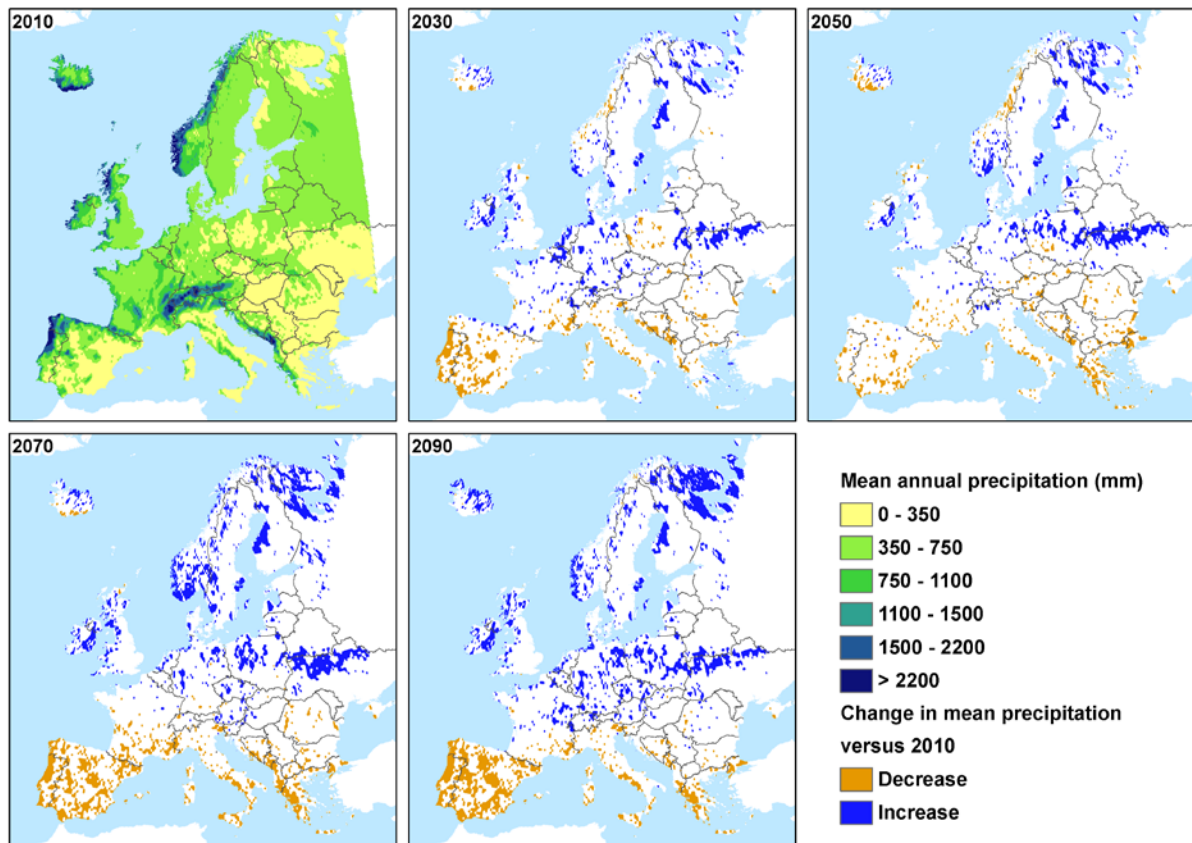
Figure 3-3: Change in annual precipitation in Europe until 2090 relative to the 2010 situation. There is a clear trend to decrease of precipitation in the Mediterranean areas.

3.3   POPULATION

The population data for Europe, produced by IIASA, reproduce the results from the GRUMP dataset for the year 2010 (used for the risk assessment in D2.10) reasonably well. The accuracy of future scenarios will decrease with time into the future. One can see from the data, that the number of pixels with no data is increasing in the future scenarios. These missing pixels in the future predictions are model artifacts. This will have a significant influence on the results of the risk analysis, especially if the no data pixels coincidence with larger cities.

Figure 2-3 show the population density in year 2010 and the change in relation to 2010 for the years 2030, 2050, 2070 and 2090. It can clearly be seen that there is a migration of people from east to west and from rural to urban areas. The total number of people in Europe is stable or slightly increasing (2000: 667 million; 2100: 676 million).

3.4   HAZARD

Landslide hazard was modeled for five situations from 2010 to 2090. Figure 3-4 shows the results obtained for changing precipitation and land cover. Changes in spatial variation landslide hazard are difficult to point out and the general pattern of landslides in Europe is the same due to the dominance of the topography in the modeling. Therefore, Figure 3-7 was prepared to show where positive and negative changes in European landslide hazard are expected to occur. Most significant changes can be observed in areas with less dominant topography such as central Germany, the central part of Romania and western UK. In most cases theses changes are from nil to low hazard, such that the general increase is low.

In total 390 000 km^2 of Europe are exposed in 2010 and this increases by 1.5% until 2090. This increase in mainly caused by changes in the precipitation pattern. The largest increase can be noted from 2070 to 2090 where the exposed area will increase by 0.8% relative to the 2010 situation. This is also the period with the highest model uncertainty due to the temporal distance to the present situation. The countries with the highest change of landslide exposed land area are the small countries of San Marino, Macedonia and Malta. In total numbers, Russia (11 500 km^2), Germany (11 000 km^2) and France (10 000 km^2) score highest on the ranking. Few countries can register a decrease in exposed area. Bosnia and Herzegovina and Montenegro have respectively a decrease of 3.2% and 0.5%. Again, a change of precipitation is the most likely reason for these changes.
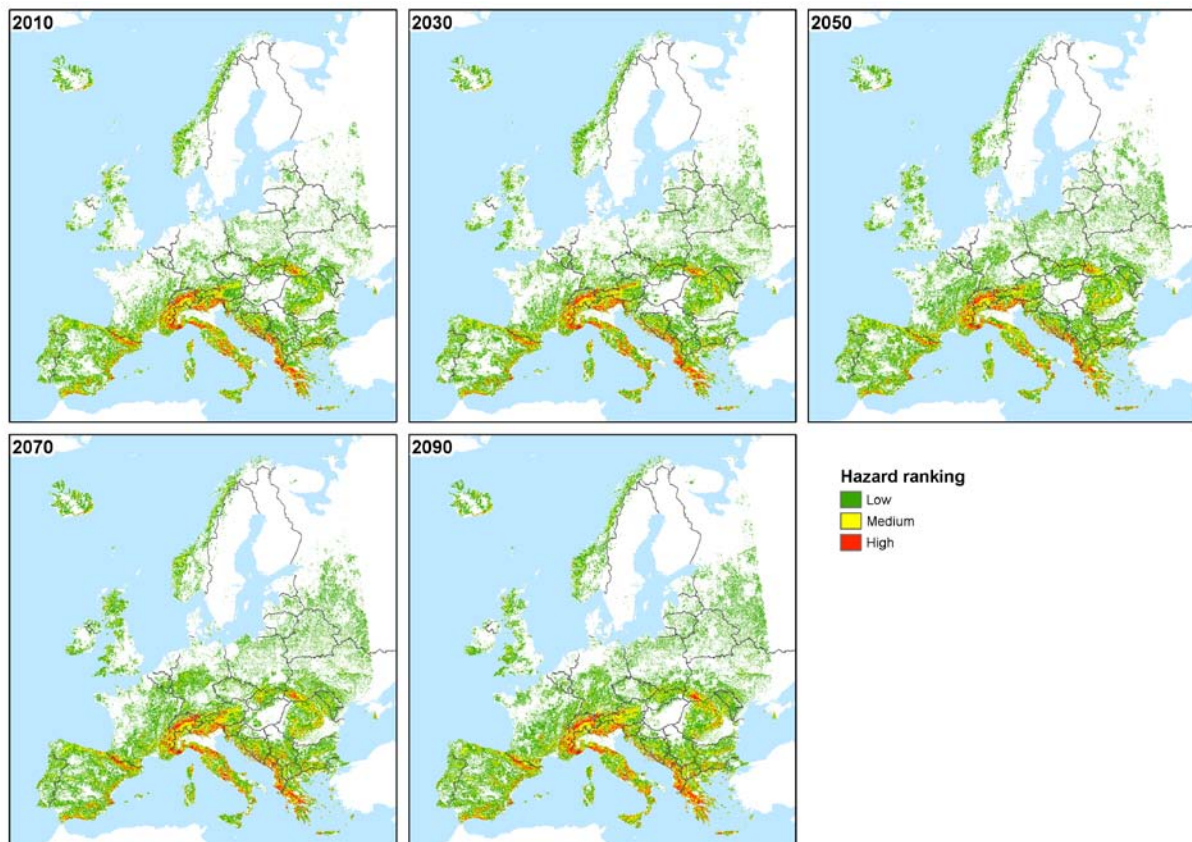
Figure 3-4: Results from the hazard model for the five time steps from 2010 to 2090. Changes are difficult to observe.
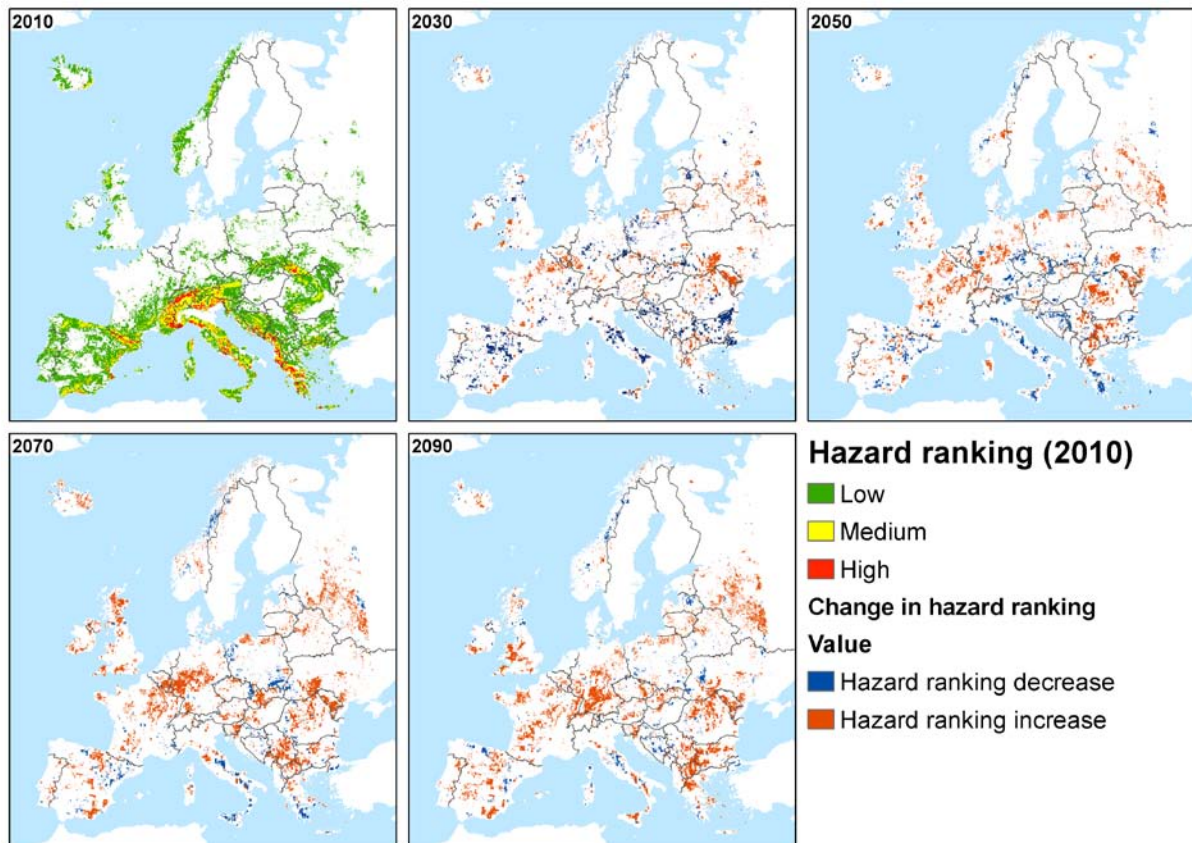
Figure 3-5: Changes in European landslide hazard 2010 until 2090. In total, landslide exposed areas increase by 1.5%. Most significant changes can be observed in areas with less dominant topography such as central Germany, the central part of Romania and western UK.

3.5   RISK

The number of people exposed to landslide hazard was used as a proxy for landslide risk. For this purpose the number of inhabitants was counted in each hazard class and the results were weighted with respect to the total number of exposed people per country (Figure 3-6).
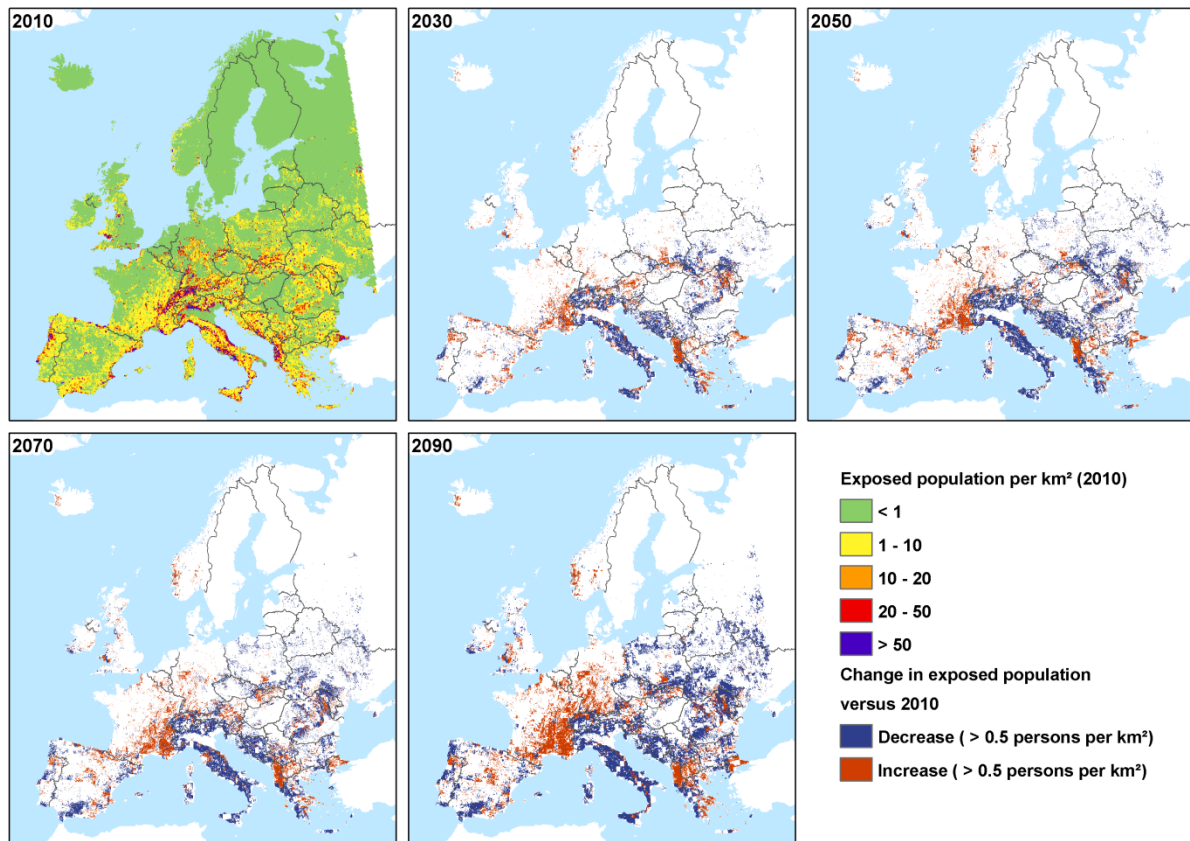
Figure 3-6: Exposed population in 2010 and the positive or negative change until 2090. Changes are mostly due to changes in the population pattern in Europe.

In total 22.3 million Europeans are currently exposed to landslide hazard in Europe. This value represents 3.8 % of the total population and will increase to 4.5% in 2090. The major part of this increase is taking place between 2070 and 2090 where model results uncertainties are already quite high. The country with the highest total number of exposed people is Italy with 6.6 million (Figure 3-7). This amounts to 11.5% of Italy's population. Italy is one of the countries where exposure is actually expected to decrease by -0.9% of the total population. The countries with the highest increase are Albania (6.1%), Macedonia (11.0%) and Malta (13.0%). In total numbers, the increase is largest in Germany followed by France. Generally the decrease is lower with -2.2% in Bosnia and -1.1% in Croatia. Again, in absolute numbers in Italy the number of exposed persons will be 1.65 million persons lower in 2090 compared to the situation in 2010. At the same time, Italy loses 22% of its population. The increase in Germany amounts to 1.72 million more than today followed by France. Here mostly areas in the central hilly areas are affected. In total, the number of exposed persons is expected to increase with 5.28 million people by 2090.
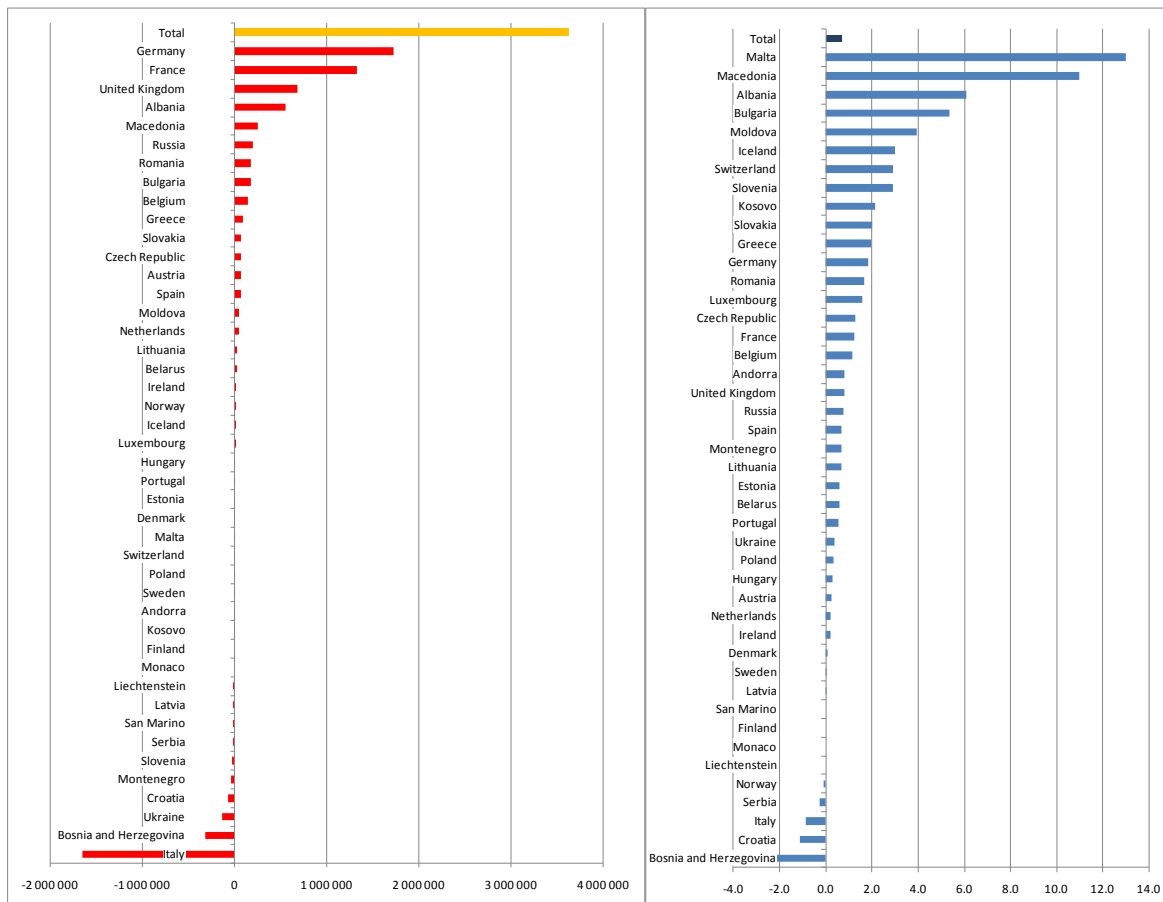
Figure 3-7: Absolute and relative changes of European population exposed to landslides from 2010 to 2090.

The comparison of the relative changes of landslide exposed area and population shows that most of the changes are caused by climate related changes in the precipitation pattern (Figure 3-8). In a few countries such as Italy and Serbia, the exposed population decreases while the exposed areas increase. Here the demographic changes dominate over the precipitation induces changes.
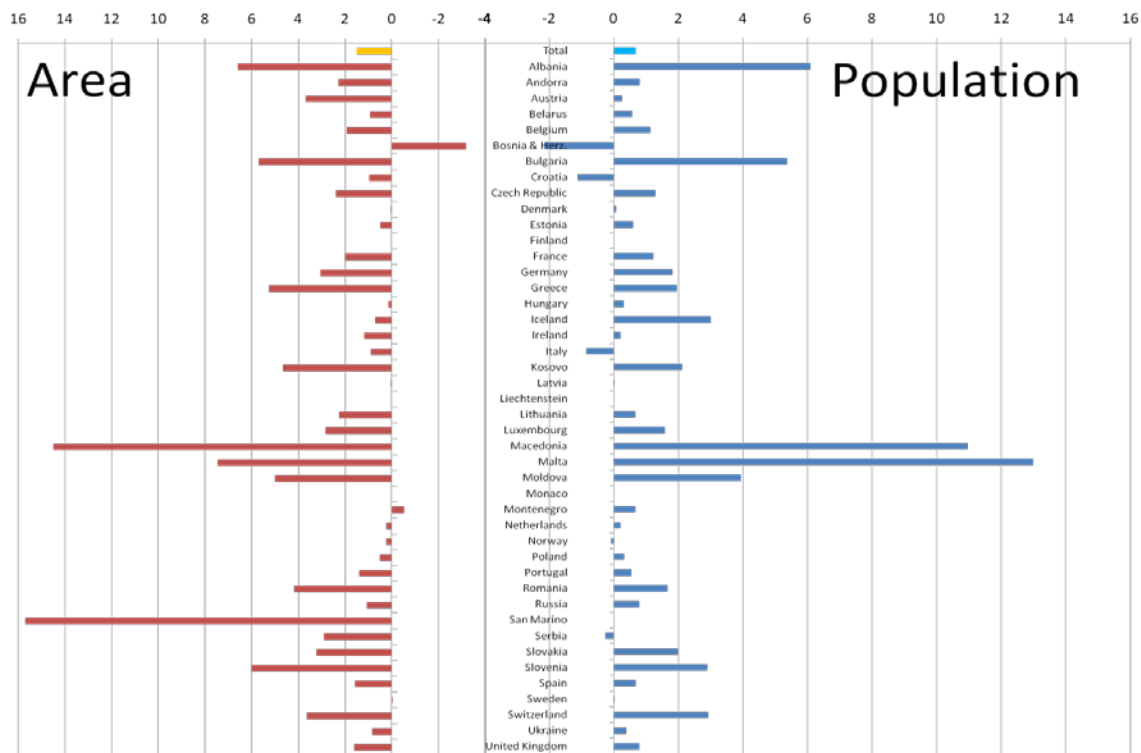
Figure 3-8: Comparison of the relative changes of landslide exposed area (red) and population (blue) in Europe 2010 – 2090.

Compared to the 2010 situation, the population exposed to landslides in Europe increases, while the total population decreases (Figure 3-9).
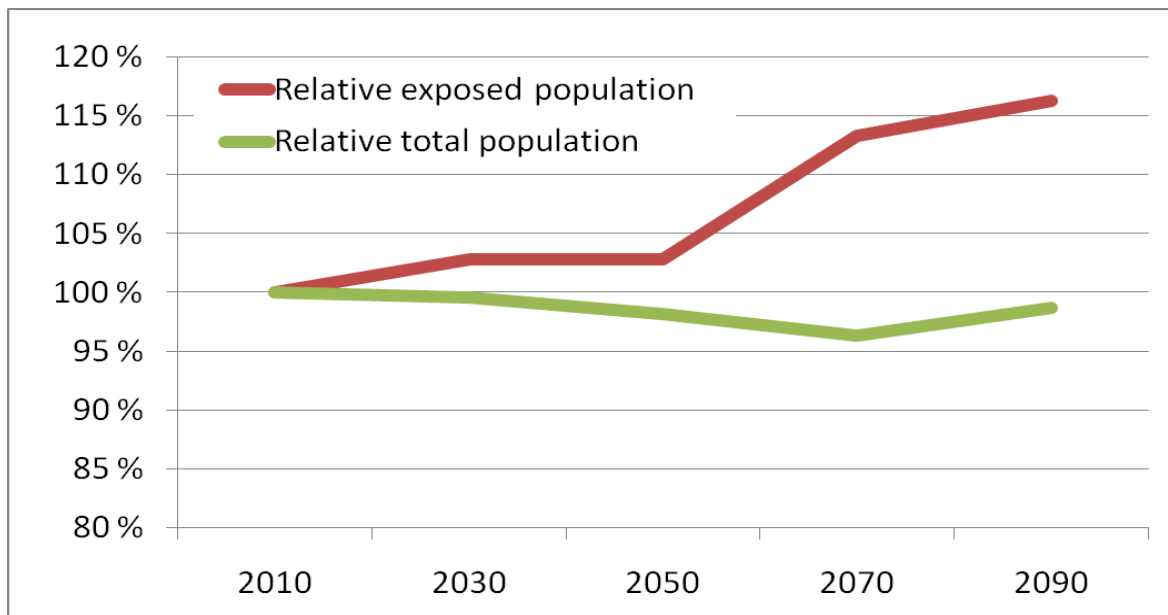
Figure 3-9: Development of the landslide exposed and total population relative to the 2010 situation.

4   DISCUSSION

Earlier studies in the Safeland project (D2.10) have shown that approximately 3.5 – 7.0 million Europeans are exposed to landslide hazard. The analysis also showed that Italy is the country with the highest number of exposed people and land area. While the most important factors for landslide susceptibility, i.e. terrain and geology, are assumed not to change within the next 100 years, precipitation, land cover and population are likely to alter under the influence of a changing climate and changing economic development. For future preparedness and mitigation of landslide hazard and risk, an analysis based on a climate change scenario can give reasonable support.

The trends in the three altering datasets are can be summarized as:
-    More and extremer precipitation in the northern parts of Europe
-    Less, but extremer precipitation in the southern parts of Europe
-    Farmland is turned into forests and grasslands, and cities will grow
-    The population in western Europe grows, mostly in the urban areas

In the present study new datasets for precipitation, population and land cover have been used. This led to significant differences from the results achieved in work package D2.10. It is therefore not relevant to compare the total numbers of exposed area and population. Focus of this study is the relative change from year 2010 to 2090 and the results give a good indication to answer this question.

The estimation of extreme precipitation is based on a physically-based climate model that actually calculates short term precipitation. For the control run 1981 to 2000 this gives a better dataset for the precipitation than the monthly extremes used in D2.10. On the other hand, the land cover and population data were less detailed then in the D2.10 model. There is a tradeoff between details and quality of the data on the one side, and homogenous datasets that are available for future scenarios on the other. The data accuracy will decrease with time and model results for the end of the model period should be interpreted with care.

The presented results for landslide hazard and risk evolution in Europe the next 80 years show a moderate increase in the exposed population. This result is in no way alarming. Landslides pose today a significant problem for many countries. The society has problems to mitigate the present problems. The increase by 0.7% of the total exposed population will not require a significant increase in mitigation efforts, provided that the present day situation with respect to mitigation efforts is adequate. If the European society manages to mitigate the present day landslide problems, Europe will be well prepared for the anticipated future changes.

5   CONCLUSIONS

European-scale analysis of present and future landslide hazard and risk required many simplifications. While detailed datasets of geology, land cover, precipitation and population are available for many selected areas in Europe, homogenous datasets that cover all of Europe with the same accuracy are rare. This problem is increasing significantly when the datasets have to cover not only the present day situation, but also the future development. The climate model results used in this study are based on a physical climate model and have a reasonable development of uncertainties in the future predictions. On the other hand, land cover and population datasets are secondary products based on climate simulations and economical modeling, which naturally include more errors in the process and are far more uncertain. In this context, the predicted changes in landslide hazard and risk in Europe, although certainly indicative, have to be investigated with care.

Nevertheless, the results from this study are useful for a prognosis of the landslide hazard and risk in next 80 years in Europe. In total, the change affects about 0.7% of the total population. This increase has to be seen in comparison to other climate change imposed challenges the next 80 years (e.g. flooding, drought). Ten countries can still expect some significant changes of more than 2% increase in exposed population. Most of these countries have significant challenges to cope with the landslide risk already today.

Landslide hazard threatens today about 3.8% of the European citizens. The mitigation of these problems is a significant challenge already today and should be continued with all available efforts. The slight increase expected for the next 80 years will not change this situation significantly. If all mitigation efforts against landslides that are necessary today are implemented, Europe will be very well prepared for the expected future changes in landslide hazard and risk.

6   REFERENCES

Fischer, G, Shah, M, van Velthuizen, H. 2002. Climate change and agricultural vulnerability, Special Report to the UN World Summit on Sustainable Development, Johannesburg, I1ASA, Laxenburg

IPCC, 2007. Climate Change 2007: Synthesis Report. (http://www.ipcc.ch/pdf/assessment-report/ar4/syr/ar4_syr.pdf)

Jacob, D. 2001: A note to the simulation of the annual and inter-annual variability of the water budget over the Baltic Sea drainage basin. *Meteorology and Atmospheric Physics*, 77, 1-4, 61-73.

Jacob, D, Andrae, U, Elgered, G, C. Fortelius, L. P. Graham, S. D. Jackson, U. Karstens, Chr. Koepken, R. Lindau, R. Podzun, B. Rockel, F. Rubel, H.B. Sass, R.N.D. Smith, B.J.J.M. Van den Hurk, X. Yang, 2001: A Comprehensive Model Intercomparison Study Investigating the Water Budget during the BALTEX-PIDCAP Period. *Meteorology and Atmospheric Physics*, 77, 1-4, 19-43.

Jaedicke, C., Van Den Eeckhaut, M., Nadim, F., Hervás, J., Kalsnes, B., Smith, J., Tofani, V., Ciurean, R., Winter, M.G. 2011. Identification of landslide hazard and risk "hotspots" in Europe. Geophysical Research Abstracts, Vol. 13, EGU2011-10398

Nadim, F, Kjekstad, O, Peduzzi, P, Herold, C, Jaedicke, C, 2006. Global landslide and avalanche hazard and risk hotspots, Landslides, 3 (2): 159-173

New, M.N, Hulme, M, Jones, P.O. 1998. Representing 20th Century space --time climate variability, Development of a 1961 --1990Mean Monthly Terrestrial Climatology, Journal of the Climate

Tubiello FN, Fischer, G. 2007. Reducing climate change impacts on agriculture: Global and regional effects of mitigation, 2000-2080. *Technological Forecasting & Social Change (Special Issue: Greenhouse Gases - Integrated Assessment)*, 74(7)1030-1056.

7 APPENDIX A: RESULT TABLES FROM THE SIMULATIONS

Table A1: European land area (km²) exposed to landslide hazard for 2010, 2030, 2050, 2070 and 2090

Name of country		Exp. Area. 2010	Exp. Area. 2010 %	Exp. Area. 2030	Exp. Area. 2030 %	Exp. Area. 2050	Exp. Area. 2050 %	Exp. Area. 2070	Exp. Area. 2070 %	Exp. Area. 2090	Exp. Area. 2090 %	Change 2010-2090	Change 2010-2090 %
Albania		10 574	36.9	11 641	40.7	10 453	36.5	11 246	39.3	12 462	43.5	1 889	6.6
Andorra		106	23.2	112	24.6	86	18.8	100	21.8	117	25.5	10	2.3
Austria		14 183	16.9	16 968	20.2	14 615	17.4	17 414	20.8	17 276	20.6	3 092	3.7
Belarus		2 875	1.4	4 656	2.3	4 545	2.2	6 025	2.9	4 792	2.3	1 917	0.9
Belgium		352	1.2	1 088	3.6	760	2.5	1 465	4.8	946	3.1	594	1.9
Bosnia and Herzegovina		10 858	21.3	9 457	18.5	9 199	18.0	10 751	21.1	9 240	18.1	-1 618	-3.2
Bulgaria		9 676	8.6	7 645	6.8	11 762	10.5	12 426	11.1	16 054	14.3	6 377	5.7
Croatia		8 084	14.4	7 054	12.5	7 930	14.1	8 620	15.3	8 624	15.3	540	1.0
Czech Republic		2 825	3.6	3 123	4.0	2 208	2.8	3 653	4.6	4 696	6.0	1 871	2.4
Denmark		61	0.1	47	0.1	163	0.4	216	0.5	76	0.2	15	0.0
Estonia		242	0.5	205	0.5	310	0.7	160	0.4	461	1.0	220	0.5
Finland		1	0.0	0	0.0	1	0.0	0	0.0	2	0.0	1	0.0
France		42 932	7.8	45 069	8.2	48 853	8.9	49 598	9.0	53 740	9.8	10 808	2.0
Germany		9 182	2.6	10 442	2.9	13 890	3.9	17 756	5.0	20 083	5.6	10 901	3.1
Greece		31 053	24.1	33 136	25.8	29 327	22.8	32 099	25.0	37 816	29.4	6 763	5.3
Hungary		1 097	1.2	1 043	1.1	978	1.1	2 343	2.5	1 237	1.3	141	0.2
Iceland		7 298	7.1	7 380	7.2	6 659	6.5	8 466	8.3	8 017	7.8	719	0.7
Ireland		1 445	2.1	1 954	2.8	2 040	2.9	2 759	4.0	2 263	3.3	817	1.2
Italy		68 032	22.8	65 186	21.9	61 881	20.8	68 455	23.0	70 735	23.7	2 703	0.9
Kosovo		1 291	11.8	1 004	9.2	1 162	10.6	2 361	21.6	1 798	16.5	507	4.7
Latvia		1 036	1.6	1 217	1.9	1 123	1.7	1 247	1.9	1 064	1.7	28	0.0
Liechtenstein		87	56.4	87	56.4	87	56.4	87	56.4	87	56.4	0	0.0
Lithuania		356	0.5	1 340	2.1	1 070	1.6	1 283	2.0	1 826	2.8	1 471	2.3
Luxembourg		25	1.0	176	6.8	70	2.7	205	8.0	98	3.8	73	2.8
Macedonia		2 313	9.3	3 099	12.5	3 521	14.2	3 937	15.9	5 907	23.8	3 594	14.5
Malta		6	9.7	9	14.7	10	17.1	7	12.4	10	17.1	5	7.5
Moldova		1 839	5.4	3 715	11.0	3 177	9.4	3 649	10.8	3 528	10.4	1 689	5.0
Monaco		7	76.7	7	76.7	7	76.7	7	76.7	7	76.7	0	0.0
Montenegro		4 145	31.2	4 095	30.8	4 152	31.3	5 053	38.1	4 077	30.7	-69	-0.5
Netherlands		28	0.1	187	0.5	101	0.3	204	0.6	116	0.3	88	0.2
Norway		11 241	3.5	10 538	3.3	12 248	3.8	11 801	3.6	12 006	3.7	765	0.2
Poland		9 342	3.0	8 594	2.8	11 031	3.5	9 837	3.2	10 957	3.5	1 615	0.5
Portugal		6 346	7.2	6 315	7.1	6 893	7.8	7 384	8.3	7 574	8.6	1 229	1.4
Romania		18 446	7.8	21 413	9.0	24 102	10.1	26 793	11.3	28 348	11.9	9 902	4.2
Russia		4 441	0.4	9 198	0.9	11 115	1.0	13 593	1.3	16 087	1.5	11 646	1.1
San Marino		18	30.5	18	30.5	11	18.8	27	46.2	27	46.2	9	15.7
Serbia		3 852	4.9	3 875	5.0	5 062	6.5	8 030	10.3	6 120	7.9	2 268	2.9
Slovakia		4 056	8.3	4 296	8.8	4 628	9.4	6 594	13.4	5 637	11.5	1 581	3.2
Slovenia		3 106	15.6	3 889	19.5	4 194	21.0	4 760	23.8	4 302	21.6	1 196	6.0
Spain		58 389	11.7	54 091	10.9	55 552	11.2	62 223	12.5	66 197	13.3	7 808	1.6
Sweden		473	0.1	252	0.1	755	0.2	758	0.2	413	0.1	-61	0.0
Switzerland		14 576	35.2	14 462	35.0	15 624	37.8	15 525	37.5	16 084	38.9	1 508	3.6
Ukraine		17 553	3.7	22 224	4.7	20 151	4.3	23 873	5.1	21 451	4.5	3 898	0.8
United Kingdom		7 524	3.1	7 808	3.2	9 292	3.8	12 743	5.3	11 442	4.7	3 918	1.6
Total		391 371	5.7	408 112	6.0	420 797	6.2	475 529	7.0	493 800	7.3	102 430	1.5

Table A2: European population exposed to landslide hazard for 2010, 2030, 2050, 2070 and 2090

Name of country		Exp. Pop. 2010	Exp. Pop. 2010 %	Exp. Pop. 2030	Exp. Pop. 2030 %	Exp. Pop. 2050	Exp. Pop. 2050 %	Exp. Pop. 2070	Exp. Pop. 2070 %	Exp. Pop. 2090	Exp. Pop. 2090 %	Change 2010-2090	Change 2010-2090 %
Albania		1 065 595	33.2	1 327 220	36.2	1 360 784	35.1	1 484 638	36.7	1 623 755	39.3	558 160	6.1
Andorra		7 420	12.2	7 817	12.2	7 446	11.2	7 569	11.0	9 258	13.0	1 838	0.8
Austria		680 611	8.2	810 051	9.7	692 405	8.4	732 484	9.1	754 365	8.5	73 754	0.3
Belarus		105 379	1.1	137 685	1.4	106 403	1.2	171 586	2.1	129 964	1.6	24 585	0.6
Belgium		39 797	0.4	192 490	1.8	128 627	1.2	239 451	2.1	181 273	1.5	141 476	1.1
Bosnia and Herzegovina		712 760	18.6	572 099	17.0	474 168	16.5	456 800	17.8	393 955	16.4	-318 805	-2.2
Bulgaria		340 614	4.6	221 809	3.5	370 373	6.7	320 778	6.1	516 645	9.9	176 031	5.4
Croatia		289 529	6.7	232 866	5.7	247 064	6.4	223 753	5.9	219 884	5.6	-69 645	-1.1
Czech Republic		257 741	2.5	264 973	2.6	175 433	1.8	326 496	3.6	332 641	3.8	74 900	1.3
Denmark		6 640	0.1	4 675	0.1	16 046	0.3	13 991	0.3	10 779	0.2	4 139	0.1
Estonia		3 971	0.4	4 439	0.4	7 111	0.8	3 330	0.4	8 615	1.0	4 644	0.6
Finland		0	0.0	0	0.0	0	0.0	0	0.0	0	0.0	0	0.0
France		2 073 376	3.4	2 542 169	3.9	2 976 108	4.4	2 939 946	4.3	3 406 176	4.7	1 332 800	1.2
Germany		1 156 229	1.4	1 332 282	1.6	1 794 769	2.1	2 663 425	3.2	2 883 888	3.2	1 727 659	1.8
Greece		1 003 338	9.9	1 006 368	10.1	794 027	8.1	865 498	9.5	1 097 498	11.9	94 160	2.0
Hungary		74 401	0.8	45 016	0.5	45 519	0.5	142 376	1.8	83 847	1.1	9 446	0.3
Iceland		10 980	3.7	21 841	6.6	12 385	3.6	23 649	6.7	24 234	6.7	13 254	3.0
Ireland		33 266	0.8	75 664	1.7	51 109	1.0	85 889	1.7	53 796	1.0	20 530	0.2
Italy		6 043 872	11.5	5 145 345	10.5	4 641 899	10.2	4 741 184	11.4	4 390 753	10.7	-1 653 119	-0.9
Kosovo		144 919	7.4	103 045	5.6	110 706	6.5	185 924	11.5	145 720	9.5	801	2.1
Latvia		22 619	1.0	26 633	1.3	21 429	1.1	23 124	1.2	18 762	1.0	-3 857	0.0
Liechtenstein		15 007	100.0	14 874	100.0	14 673	100.0	14 473	100.0	14 339	100.0	-668	0.0
Lithuania		14 301	0.4	43 924	1.3	35 088	1.1	40 374	1.1	45 870	1.1	31 569	0.7
Luxembourg		0	0.0	16 766	3.1	7 721	1.2	33 635	4.8	11 812	1.6	11 812	1.6
Macedonia		102 208	4.8	158 339	7.1	198 142	8.7	207 501	9.2	359 901	15.8	257 693	11.0
Malta		3 002	10.0	6 901	23.0	6 901	23.0	3 002	10.0	6 901	23.0	3 899	13.0
Moldova		190 487	4.4	396 081	10.0	274 323	7.9	297 349	9.5	236 561	8.3	46 074	3.9
Monaco		39 026	86.1	39 026	86.1	39 026	86.1	39 026	86.1	39 026	86.1	0	0.0
Montenegro		166 180	28.4	138 443	25.8	127 468	25.8	152 390	33.4	125 339	29.1	-40 841	0.7
Netherlands		6 354	0.0	73 432	0.4	32 067	0.2	67 672	0.4	49 705	0.3	43 351	0.2
Norway		99 790	2.3	85 606	1.8	109 829	2.2	121 197	2.3	118 335	2.2	18 545	-0.1
Poland		743 470	1.9	687 355	1.8	799 849	2.2	669 559	2.0	746 619	2.2	3 149	0.3
Portugal		640 264	7.0	649 221	7.1	586 100	6.5	622 419	7.3	649 042	7.5	8 778	0.5
Romania		866 692	3.9	925 068	4.4	1 016 354	5.1	1 106 020	5.9	1 048 333	5.6	181 641	1.7
Russia		192 992	0.6	287 374	0.9	292 640	1.0	280 464	1.0	394 889	1.4	201 897	0.8
San Marino		7 154	30.0	4 976	30.0	1 088	10.0	2 015	30.0	1 233	30.0	-5 921	0.0
Serbia		193 746	2.3	132 668	1.6	166 617	1.9	291 134	3.4	180 914	2.1	-12 833	-0.3
Slovakia		246 007	4.7	277 969	5.3	281 987	5.5	342 980	7.1	321 165	6.7	75 158	2.0
Slovenia		218 756	11.0	275 495	15.2	213 846	13.3	219 309	15.8	188 212	13.9	-30 544	2.9
Spain		2 115 056	5.7	2 113 235	5.7	2 076 390	5.7	2 258 434	6.6	2 181 315	6.4	66 259	0.7
Sweden		355	0.0	846	0.0	3 852	0.0	9 993	0.1	2 241	0.0	1 887	0.0
Switzerland		991 055	14.2	936 949	14.2	940 839	15.5	907 269	15.6	994 916	17.2	3 861	2.9
Ukraine		789 561	2.3	943 841	3.1	699 971	2.6	842 378	3.3	659 861	2.7	-129 700	0.4
United Kingdom		563 212	1.0	622 744	1.0	938 153	1.5	1 061 596	1.6	1 242 390	1.8	679 178	0.8
Total		22 277 731	3.8	22 905 619	3.9	22 896 732	4.0	25 242 078	4.5	25 904 726	4.5	3 626 995	0.7

8   APPENDIX B: DESCRIPTION OF THE ICG MODEL

8.1   ICG MODEL

The ICG model is based on the experience gained in the HOTSPOT study from 2006. This type of analysis is based on expert judged reclassification and weighting of different factors that are assumed to be important for landslide susceptibility and hazard. Once the hazard is established, risk is estimated by considering exposure and vulnerability.

The analysis is a pixel based multiplication of the important factors to achieve a hazard index. This is done independently for two triggers, rainfall and seismicity.

8.1.1   Model for Landslide Hazard Evaluation
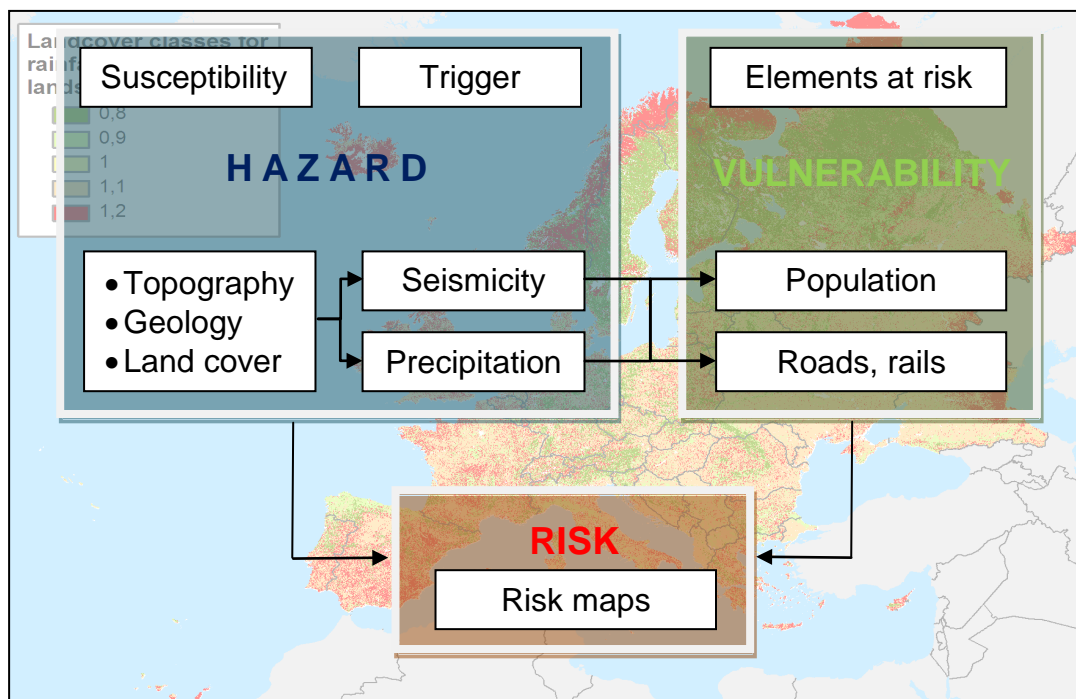
Figure 8-1: Schematic approach for landslide hazard and risk evaluation.

The term "landslide" in this study focuses on events involving gravity-driven rapid mass movement down-slope, like rockslides, debris flows, and rainfall- and earthquake-induced slides; which pose a threat to human life. Slow moving slides have significant economic consequences for constructions and infrastructure, but rarely cause any fatalities.

To identify the global landslide hazard and risk "hotspots", Nadim et al. (2006) adopted a simplified first-pass analysis method. The scale of their analysis was a grid of roughly 1km x 1km pixels where landslide hazard, defined as the annual probability of occurrence of a potentially destructive landslide event, was estimated by an appropriate combination of the triggering factors (mainly extreme precipitation and seismicity) and susceptibility factors (slope, lithology, vegetation and landcover). The principles of the method are depicted in Figure 8-1.

The weights of different triggering and susceptibility factors were calibrated to the information available in landslide inventories and physical processes. The general approach used in the present study is a modified and improved version of the approach used by Nadim et al. (2006).

One of the key improvements in the present model is the increased resolution on the DEM and consequently the slope data. In previous studies a 30 arc second resolution was used, whereas the present study uses the 3 arc seconds SRTM dataset.

The hazard maps are divided in precipitation-induced landslide hazard and earthquake-induced landslide hazard. The landslide hazard indices were estimated using the following equations:

$$H_r = (S_r \times S_l \times S_v) \times T_p \qquad\qquad (1)$$
$$H_e = (S_r \times S_l \times S_v) \times T_s \qquad\qquad (2)$$

where H_r and H_e are landslide hazard indices for rainfall and earthquake-induced landslides respectively, S_r is the slope factor within a selected grid, S_l is lithological (or geological) conditions factor, S_v is the vegetation cover factor T_p is the precipitation factor and T_s describes the seismic conditions.

The population exposure maps where calculated using the following equations

where *POP* is population and $H_{r,ref}$ and $H_{e,ref}$ are normalization factors allowing categorization of the exposure data.

8.1.2   Data preparation

Most of the available input data needs a thorough preparation before it can be used in a GIS analysis. The method calculates hazard and risk pixel by pixel and all data has to be regridded to the available grid size of the underlying digital elevation model. In the case of this analysis, south of 60° north, the resolution is 3 arc seconds, north of 60° another dataset had to be used that yields only 30 arc seconds resolution.

8.1.3   Slope factor S_r

The slope factor represents the natural landscape ruggedness within a grid unit. In February 2000, NASA collected elevation data for much of the world using a radar instrument aboard

the Space Shuttle. The raw data collected on the mission were processed over three years. NASA has now released a global elevation dataset called SRTM3, referring to the name of the mission and the resolution of the data, which is 3 arc-seconds, or approximately 90 by 90 m per data sample near the equator. The SRTM3 data set covers the globe from 60 degrees south latitude to 60 degrees north latitude. The vertical accuracy is estimated such that 90% of posts are within 16m tolerance of the actual position.

North of 60 degrees a different dataset had to be used. We chose the GTOPO dataset with a resolution of roughly 1 x 1 km.

The SRTM and N50 slope angle data are classified into hazard classes as shown in columns 1 through 3 in Table 8-1 below. In order to make a corresponding hazard classification for the GTOPO slope angle data (which have a pixel area of 100 times the SRTM and N50 data), two test areas have been identified where SRTM/N50 slope angle data are compared to GTOPO slope angle data:

1. Norway (N50 data compared to GTOPO data)
2. Southern Europe: Mainly Alps and Balkans (SRTM data compared to GTOPO data)

In Figure 8-2 and Figure 8-3 are shown histograms for each of these two test areas comparing GTOPO slope angle data to N50 data (Norway) and SRTM data (Southern Europe).
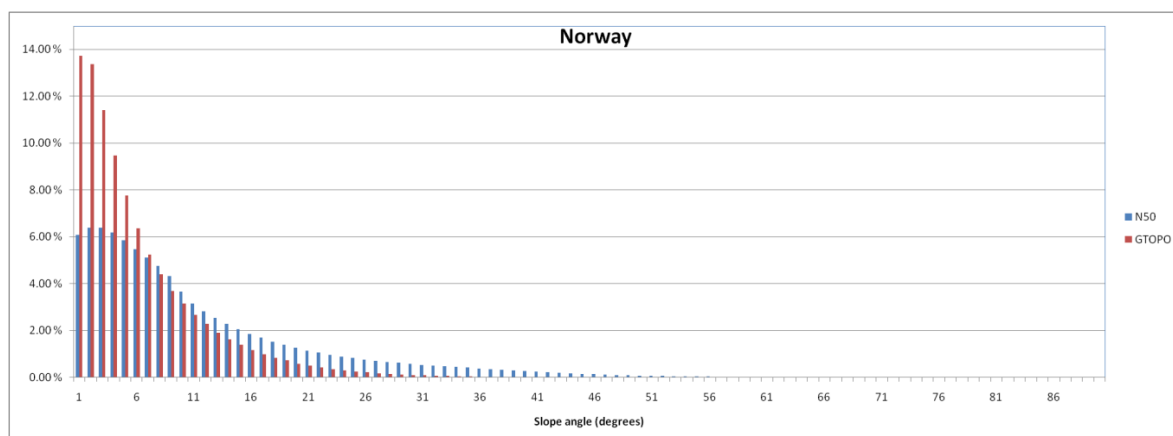
Figure 8-2: Histogram showing the percentage of land area having certain slope angle for test area 1: Norway. Comparison of GTOPO slope angle data to N50 slope angle data

Both curves show that the fine resolution data (N50 and SRTM) on average show higher slope angle than the coarser GTOPO data. The histogram data have then been used to establish slope angle ranges for each hazard class for GTOPO data (corresponding to the SRTM/N50 slope angle ranges in columns 2 and 3 in Figure 8-2). The criteria used is that for any given hazard class, the fraction of the land area belonging to this hazard class should be independent of whether SRTM/N50 or GTOPO data is used.
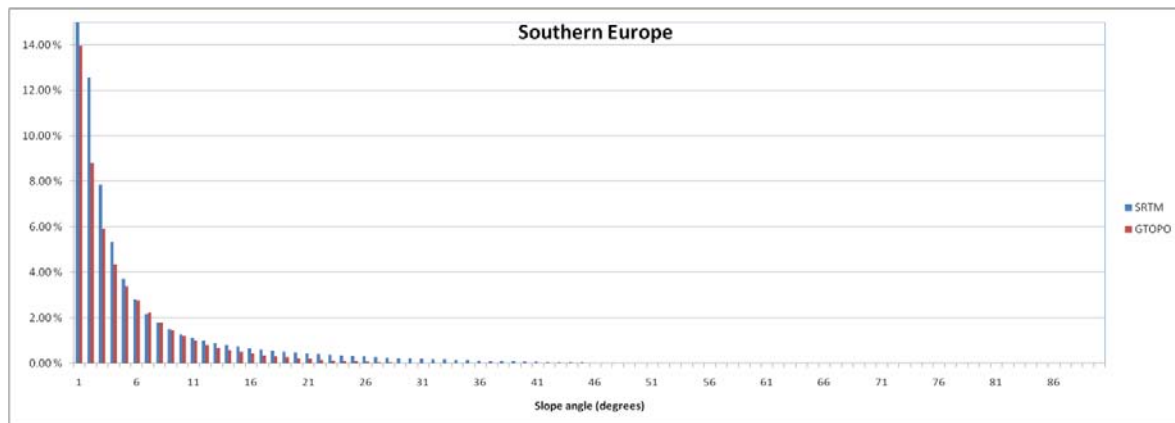
Figure 8-3: Histogram showing the percentage of land area having certain slope angle for test area 2: Southern Europe. Comparison of GTOPO slope angle data to SRTM slope angle data

The result of the analysis is shown in Table 8-1. The resulting slope angles for each of the hazard classes for GTOPO data are given in columns 4 and 5.

Columns 6 and 7 are results for test area 1 Norway.
Column 6 shows the fraction of land area belonging to each hazard class based on the N50 angle ranges from column 2 and 3.
Column 7 shows the fraction of land area belonging to each hazard class based on the GTOPO angle ranges from column 4 and 5.
Column 6 and 7 are in reasonable agreement indicating a good recalibration.

Columns 8 and 9 are results for test area 2 Southern Europe.
Column 8 shows the fraction of land area belonging to each hazard class based on the SRTM angle ranges from column 2 and 3.
Column 9 shows the fraction of land area belonging to each hazard class based on the GTOPO angle ranges from column 4 and 5.
Column 8 and 9 are in reasonable agreement, except for rows one and two. This discrepancy is believed to be of minor importance as hazard classes 0 and 1 represent low hazard levels.

Table 8-1: Slope angle ranges for each hazard class for SRTM and N50 data

S_r	Angle N50 / SRTM		Angle GTOPO		N50 Norway	GTOPO Norway	SRTM S Europe	GTOPO S Europe
	From	To	From	To	Fraction	Fraction	Fraction	Fraction
0	0	1	0	0	11.20 %	4.27 %	28.48 %	48.07 %
1	1	6	1	3	30.88 %	38.52 %	49.68 %	28.66 %
2	6	12	4	7	26.45 %	28.83 %	10.64 %	12.71 %
3	12	18	8	10	13.23 %	11.25 %	4.69 %	4.44 %
4	18	24	11	13	7.33 %	6.84 %	2.78 %	2.51 %
5	24	40	14	22	8.76 %	8.23 %	3.19 %	3.02 %
3	40	45	23	26	1.07 %	1.10 %	0.30 %	0.39 %
3	45	90	27	90	1.07 %	0.96 %	0.23 %	0.20 %

Note: for slopes which angle is less than 1° (i.e. for flat or nearly flat areas), S_r is set equal to zero because the resulting landslide hazard is zero even if the other factors are favourable.
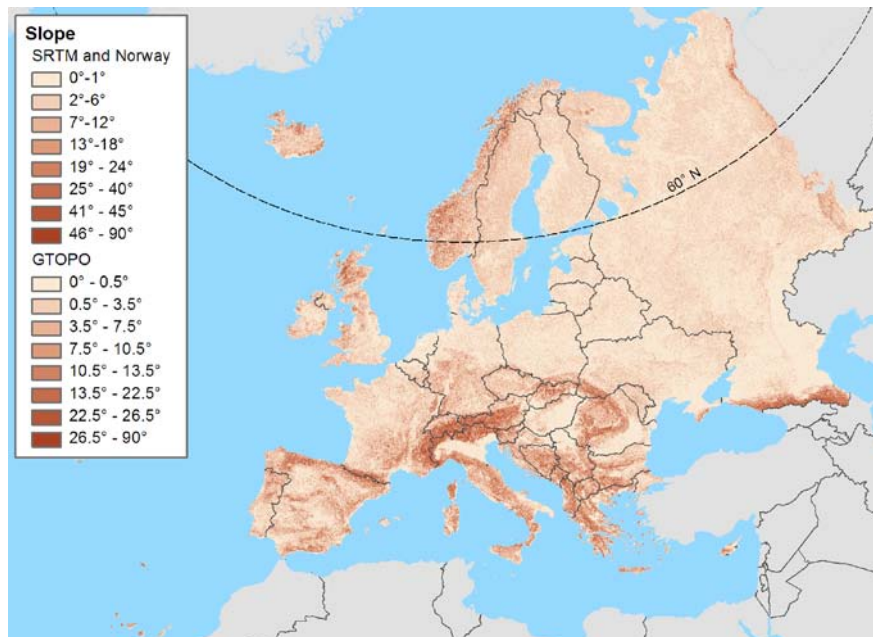
Figure 8-4: Slope factor S_r for the study area.

8.1.4 Lithology factor S_l

This is probably the most difficult parameter to assess. Ideally, detailed geotechnical information should be used but, at the global scale, only a general geological description is available. Rock strength and fracturing are the most important factors to evaluate lithological characteristics, and these characteristics can vary greatly over short distances.

The dataset used in the study was the Geological map of Europe at 1/5,000,000 scale published by Bundesanstalt für Geowissenschaften und Rohstoffe. The map is available on request from the institution. This map is the best geological dataset compiled at a European scale showing the geology of the whole continent, including land areas and oceans. In the map, three main types of rocks are identified: sedimentary rocks, extrusive volcanic rocks and endogenous rocks (plutonic or strongly metamorphosed).

Table 8-2: Classification of the lithology based on the European geological map.

Lithology and stratigraphy	Susceptibility	S_l
• Extrusive volcanic rocks - Precambrian, Proterozoic, Paleozoic and Archean. • Endogenous rocks (plutonic and/or metamorphic) - Precambrian, Proterozoic, Paleozoic and Archean.	Low	1
• Old sedimentary rocks - Precambrian, Archean, Proterozoic, Paleozoic. • Extrusive volcanic rocks – Paleozoic, Mesozoic. • Endogenous rocks - Paleozoic, Mesozoic, Triassic, Jurassic, Cretaceous.	Moderate	1
• Sedimentary rocks - Paleozoic, Mesozoic, Triassic, Jurassic, Cretaceous. • Extrusive volcanic rocks – Mesozoic, Triassic, Jurassic, Cretaceous. • Endogenous rocks – Meso-Cenozoic, Cenozoic.	Medium	2
• Sedimentary rocks – Cenozoic, Quaternary. • Extrusive volcanic rocks – Meso-Cenozoic.	High	3
• Extrusive volcanic rocks – Cenozoic.	Very high	3

Three susceptibility classes were used in the analyses, as shown in Table 8-2. Usually old rocks are stronger than young rocks. Plutonic rocks are usually strong and represent low susceptibility. Strength of metamorphic rocks is variable, but these rocks often have planar structures such as foliation and therefore may represent higher susceptibility than plutonic rocks. Lava rocks will usually be strong, but may be associated with tuff (weak material). Therefore, areas with recent volcanism are classified as highly susceptible. Sedimentary rocks are often weak, especially young ones.
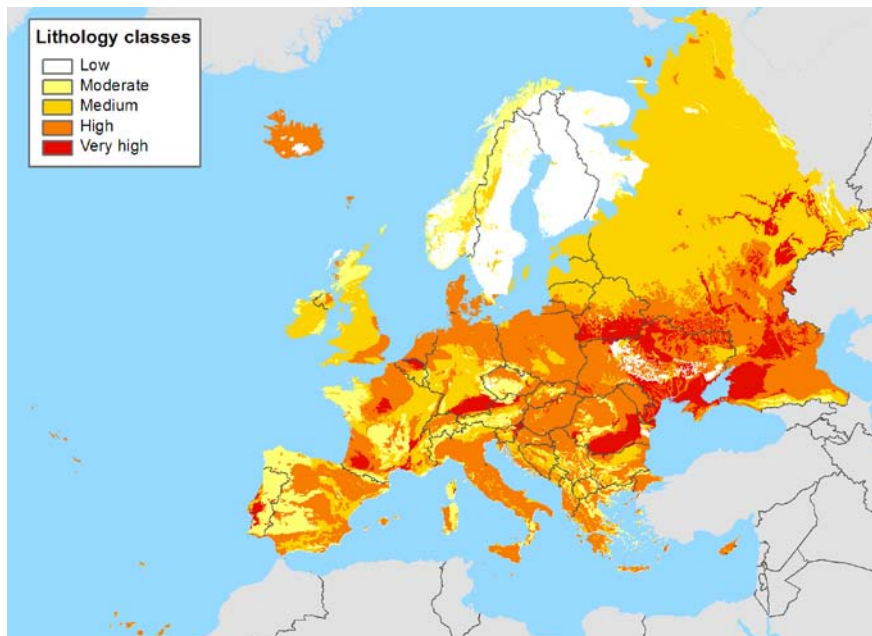
Figure8-5: Lithology factor S_l for the study area.

8.1.5   Land cover index S_v

The IIASA database has 6 different classes of land cover, which have been translated into 5 categories (scale 1 to 5) with respect to resistance to landslides. Table 8-3 shows the range of S_v for these 5 categories.

Table8-3: Classification of land cover for the hazard analysis

Land cover class	Susceptibility	S_v
Water	ignored	0
Urban	Moderate	0.5
Forest	Medium	0.9
Cropland	High	1.1
Grassland	Very high	1.2
Other (mainly barren and water)	Very high	1.2
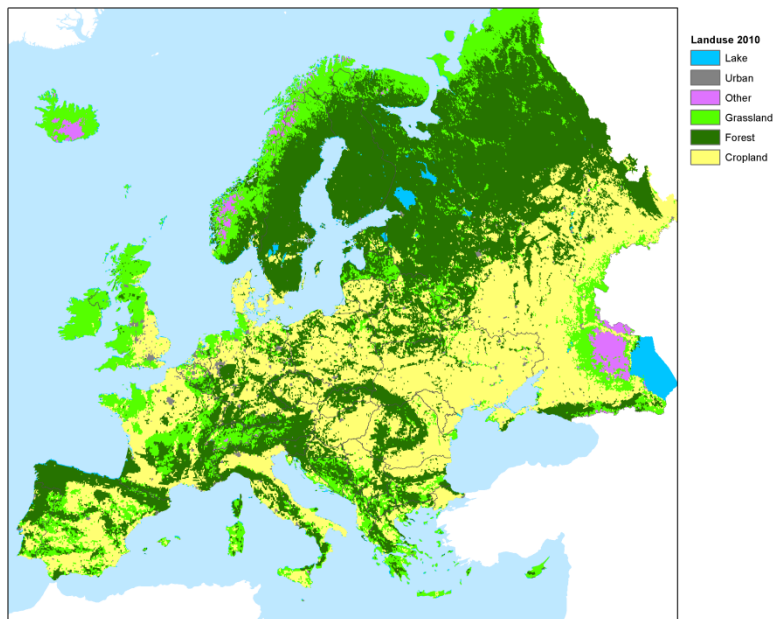
Figure8-6: Vegetation cover index Sv for precipitation-induced landslides

8.1.6   Precipitation trigger factor T_p

The categorization of T_p was based on the estimate of the 99.9% percentile of 24h precipitation for 20 year periods. This corresponds approximately to a 50 year event. The data processing procedure is described in chapter 2.1.1.

On the basis of the estimated 99.9% percentile of 24h precipitation for 20 year periods, a precipitation index T_{p1} was assigned as listed in Table 8-4.

Table 8-4: Reclassification for 99.9 % percentile of precipitation extremes in Europe

Daily (24h) precipitation in millimeters	Susceptibility	T_{p1}
0 – 60	Low	1
61 – 75	Moderate	2
76 – 95	Medium	3
96 – 120	High	4
> 120	Very high	5

8.1.7 Categorisation of landslide hazard

The obtained landslide hazard indices were calibrated against the databases of landslide events in selected (mostly European) countries to obtain the frequency of the events. On the basis of this calibration, the following landslide hazard classifications were established:

Table 8-5: Classification of the landslide hazard due to precipitation and seismicity

Values for $H_{landslide, rainfall}$	Class	Classification of landslide hazard potential	Representative annual frequency in 1 km² grid cell
≤ 2	0	Negligible	~ 0.00 %
3 – 9	1	Very low	~ 0.00 %
10 – 20	2	Low	0.01 %
21 – 36	3	Low to moderate	0.03 %
37 – 54	4	Moderate	0.10 %
55 – 74	5	Medium	0.30 %
75 – 99	6	Medium to high	1.00 %
100 – 134	7	High	3.00 %
> 134	8	Very high	10.00 %